Available online: http://journal.uir.ac.id/index.php/JEEE/index

Journal of Earth Energy Engineering

Publisher: Universitas Islam Riau (UIR) Press

Capacitance Resistance Clustered Model for Mature Peripheral Waterflood Performance Prediction & Optimization

Billal Aslam*[1,2], Hasto Nugroho[1,3], Fahriza Mahendra[1], Rani Kurnia[1,2], Taufan Marhaendrajana[1,2], Septoratno Siregar [1,2]
[1]OGRINDO Research Consortium, Institut Teknologi Bandung, Basic Science Center B Building 4th Floor Ganesha 10 Street, Bandung, West Java, Indonesia – 40132
[2]Department of Petroleum Engineering, Faculty of Mining and Petroleum Engineering, Institut Teknologi Bandung, Basic Science Center B Building 4th Floor Ganesha 10 Street, Bandung, West Java, Indonesia – 40132
[3]Medco E&P Indonesia, The Energy 53rd Fl. SCBD Lot 11A Jend. Sudirman Street Kav. 52-53, Jakarta, Indonesia-12190
*Corresponding Author: billal.aslam@itb.ac.id

Article History:

Received: October 3, 2022
Receive in Revised Form: December 6, 2022
Accepted: December 7, 2022

Keywords:

Peripheral Waterflood, Capacitance Resistance Model, Reservoir Management, Improved Oil Recovery, Mature Field

Abstract

Optimizing water injection rate distribution in waterflooding operations is a vital reservoir management aspect since water injection capacities may be constrained due to geographic location and facility limitations. Numerical grid-based reservoir simulation is traditionally used to evaluate and predict waterflood performance. However, the reservoir simulation approach can be time-consuming and expensive with the vast amount of wells data in mature fields. Capacitance Resistance Model (CRM) has been widely used recently as a data-driven physics-based model for rapid evaluation in waterflood projects. Even though CRM has a smaller computation load than numerical reservoir simulation, large mature fields containing hundreds of wells still pose a challenge for model calibration and optimization. In this study, we propose an alternative solution to improve CRM application in large-scale waterfloods that is particularly suitable for peripheral injection configuration. Our approach attempts to reduce CRM problem size by employing a clustering algorithm to automatically group producer wells with an irregular peripheral pattern. The selection of well groups considers well position and high throughput well (key well). We validate our solution through an application in a mature peripheral waterflood field case in South Sumatra. Based on the case study, we obtained up to 18.2 times increase in computation speed due to parameter reduction, with excellent history match accuracy.

INTRODUCTION

Waterflooding has been a technically and economically proven way to increase oil reserves in mature fields after primary depletion (Temizel et al., 2017; Thakur, 1991; Willhite, 1986). Field experience shows that a well-implemented waterflood can increase the oil recovery factor to 35 – 45% of its original in place (Zitha et al., n.d.). Modern waterflood asset management to ensure maximum economic value requires comprehensive technical and operational planning that needs to be continuously improved (Thakur, 1998). In waterflooding operations, one of the most essential aspects of reservoir management is optimizing the water injection rate distribution. This is necessary since water injection capacity may be limited due to the facility's location or the surrounding geography. Interwell connectivity between injection and production wells is a key component to define to gain an understanding of waterflood performance. This is because interwell connectivity strongly correlates with the waterflood sweep efficiency (Albertoni & Lake, 2003; Møyner et al., 2015).

Traditionally, numerical grid-based reservoir simulation is used for waterflood performance evaluation and prediction. Numerical reservoir simulation is regarded as the most robust approach due to its foundation in flow physics and its ability to include realistic geological assumptions. However, the reservoir simulation approach can be time-consuming and expensive with the vast amount of wells data in mature

DOI: 10.25299/jeee.2022.10633
eISSN: 2540-9352 pISSN: 2301-8097

fields. This can hinder the decision process and lead to delayed action to optimize waterflood operations. Hence, an improved method is still needed to analyze waterflood performance.

The data-driven modeling methodology has recently acquired favor in various research areas, including reservoir engineering, and fundamentally transformed the petroleum business due to recent advances in real-time sensors and computer technologies. This strategy has radically transformed the petroleum sector as a consequence. Data-driven modeling, abbreviated DDM, refers to a collection of methods that, when applied to operational data, enable the efficient computing of model predictions that are both sufficiently accurate and representative of the actual system (Balaji et al., 2018). This traits is essential for implementing the closed-loop reservoir management (CLRM), as the model need to be executed on real-time (Gildin & Lopez, 2011). DDM typically involves a machine learning (ML) algorithm to train; however, the inclusion of a physics-based model in DDM can resolve the limitation of a sole-ML-based model. This is known as the grey-box approach (Liu et al., 2021). Several data-driven grey-box models for waterflood performance prediction and optimization have been developed, such as Capacitance Resistance Model (Sayarpour et al., 2009; Yousef et al., 2006), INSIM (Guo et al., 2018; Zhao et al., 2015), and Network Models (Kiær et al., 2020; Wang et al., 2021). These methods differ in physical assumption used and implementation complexity. A detailed comparison between data-driven methods for waterflood performance evaluation is available in other works (Artun, 2017; Balaji et al., 2018). Overall, CRM is the most widely used approach due to its ease of implementation and fundamental physical basis.

An equation for the mass balance differential is derived for an injection and production system in a closed control volume, which is the foundation of the CRM model. By finding a semi-analytical solution to these differential equations, a rapid calculation can be performed in order to evaluate CRM. Constant characteristics linked to inter-well connectivity, system compressibility, and well productivity index characterize production response from the injection in the CRM. Through minimizing the model response error to historical production and bottom-hole pressure data with the actual injection rate as input, CRM parameters can be established. As a result, CRM can evaluate the effectiveness of a mature waterflood by only using a few data types and without having to first acquire an understanding of the reservoir's parameters. Albeit CRM is regarded as a simplified physics model, it has been shown to be reliable in predicting short-term waterflood performance and can be an excellent preliminary study before using detailed numerical modeling approach (Davudov et al., 2020; Sayarpour et al., 2009).

Even though CRM has a smaller computation load than numerical reservoir simulation, large mature fields containing hundreds of wells still pose a challenge for model calibration and optimization. The number of parameters to be solved simultaneously, well downtime, and data outliers have been regarded as the main factors that restrict CRM application in large-scale reservoirs (Weber et al., 2009). Several attempts have been proposed to improve CRM performance in large-scale reservoirs, including problem size reduction by removal of inactive wells and producer wells beyond the radial distance limit (Weber et al., 2009); alternative CRM formulation using Integrated Capacitance Resistance Model (Nguyen et al., 2011); and use of global optimization solvers (JAMALI & ETTEHADTAVAKKOL, 2017). However, no universal solution exists for CRM treatment in large-scale waterflood applications.

In this study, we propose an alternative solution to improve CRM application in large-scale waterfloods that is particularly suitable for peripheral injection configuration. Our approach attempts to reduce CRM problem size by employing a clustering algorithm to automatically group producer wells with an irregular peripheral pattern. The selection of well groups considers well position and high throughput well (key well). We validate our solution through an application in a mature peripheral waterflood field case in South Sumatra. The proposed method reduces computation time and provides accurate model calibration.

METHODOLOGY & FIELD CASE

Methodology

The capacitance resistance model (CRM) characterizes a flooded reservoir by estimating interwell connectivities, time constants, and productivity indices using production/injection rates for history matching. Assuming each injector and producer is represented by a particular control volume (CRM-IP), and the reservoir only contains two-phase immiscible fluid, the rate continuity for each control volume is defined as (Yousef et al., 2006).

$$\frac{dq_{ij}(t)}{dt} + \frac{1}{\tau_{ij}} q_{ij}(t) = \frac{1}{\tau_{ij}} f_{ij} i_i(t) - J_{ij} \frac{dp_{wf,j}}{dt} \quad (1)$$

where q_{ij} is the production rate of producer-j from injector-i and producer-j control volume (see Figure 2), f_{ij} is the allocation factor of injection rate that represents the contribution of injection from injector-i to producer-j, where the sum of allocation factor for each injector should not exceed one to maintain mass

Journal of Earth Energy Engineering
Vol. 11 No. 3, December 2022, pp 113-124

continuity. τ_{ij} is the time constant for each injector-producer pairs, which account for the system compressibility, i.e.,

$$\tau_{ij} = \left(\frac{c_t V_p}{J}\right)_{ij} \tag{2}$$

By assuming a constant injection rate at a specified time interval, Δt_k, and linear BHP variation, the semi-analytical solution to the ordinary differential equation of Eq. (1) for liquid production rate prediction can be written as (Sayarpour et al., 2009)

$$q_{ij}(t_k) = q_{ij}(t_{k-1}) e^{\frac{-\Delta t_k}{\tau_{ij}}} + \left(1 - e^{\frac{-\Delta t_k}{\tau_{ij}}}\right)\left[f_{ij}\, I_i^{(k)} - J_{ij}\, \tau_{ij} \frac{\Delta p_{wf}^{(k)}}{\Delta t_k}\right] \tag{3}$$

Furthermore, assuming producer wells operate at constant flowing bottom-hole pressure, as typical for producer wells with artificial lift (i.e., SRP, ESP), Eq. (3) becomes

$$q_{ij}(t_k) = q_{ij}(t_{k-1}) e^{\frac{-\Delta t_k}{\tau_{ij}}} + \left(1 - e^{\frac{-\Delta t_k}{\tau_{ij}}}\right)\left[f_{ij}\, I_i^{(k)}\right] \tag{4}$$

The total production rate for each producer is the sum of the contribution from all of the injectors, which can be expressed as

$$q_j(t) = \sum_{i=1}^{N_{inj}} q_{ij}(t) \tag{5}$$

Injection well allocation factor, f_{ij} and time constant, τ_{ij} are calibrated by minimizing the misfit between CRM production rate output (q_{est}) and observed production data (q_{obs}). We used mean squared error as the objective function to minimize, such that

$$MSE = \frac{\sum_{n=1}^{N_{data}} (q_{obs} - q_{est})^2}{N_{data}} \tag{6}$$

The empirical fractional flow model represents oil rate production in our CRM implementation. We used (Gentil, 2005) fractional flow model, which relates oil fractional flow (f_o) to cumulative water injection (W_i). This model is valid for high water cut wells ($WC > 90\%$),

$$f_o(t) = \frac{1}{1 + F_{wo}} = \frac{1}{1 + \alpha W_i^{\beta}} \tag{7}$$

Empirical constants in Eq. (7), α and β can be calibrated using the same method as liquid production rate match, but oil rate data is used instead. We applied the interior-point algorithm (Byrd et al., 1999) implemented in MATLAB *fmincon* function to obtain the model parameters ($f_{ij}, \tau_{ij}, \alpha, \beta$) that minimizes the error function (Eq. 6).

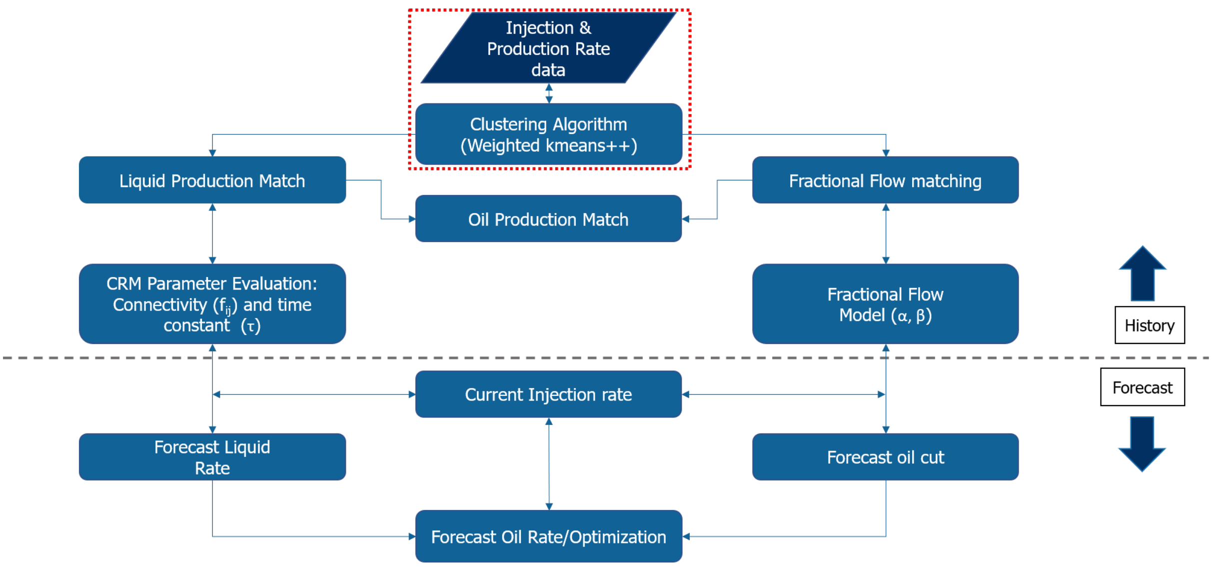

Figure 1 Workflow of CRM-IP Cluster (CRM-IPC)

Figure 1 shows our adjusted workflow of CRM-IP to implement CRM-IP with clustering (CRM-IPC). CRM-IPC essentially groups the producers into clusters that combine (sum up) all the producer rates in the same cluster at each period. The justification for this approach is that production wells will take injection contributions from temporary shut-in producer wells close to each other. Hence, this clustering method also works as a way to normalize production data. After clustering, the input data can be treated as the original CRM-IP calculation with 'less' producer well, as illustrated in Figure 2.

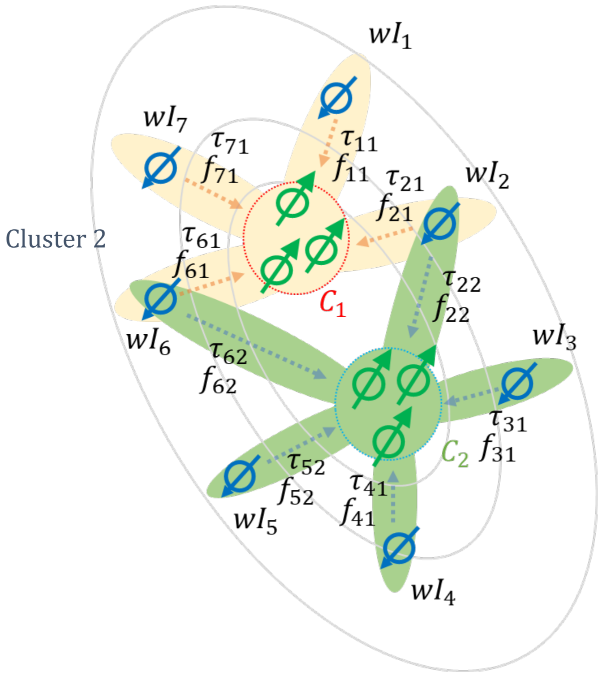

Figure 2 Illustration of injector–clustered producer pair-based control volume, CRM-IPC. Control volumes originating from the injector are permutated to all production well clusters. Grey lines represent contour depth for a typical anticline structure.

A. Optimal Cluster Center Determination

We adjust the kmeans++ algorithm (Arthur & Vassilvitskii, 2007) cluster center seeding probability by using each well average liquid production rate as weighting. This will promote the cluster centroids to be closer to the well with high liquid rates (key wells) as it should correspond to wells with higher injection allocation. The algorithm for carefully seeding the cluster center with weighting is given as follows:

Table 1. kmeans++ algorithm

Algorithm 1: Kmeans++ with weighting (Arthur & Vassilvitskii, 2007)

1. Take one center c_1, chosen uniformly at random from χ.
2. Take a new center c_i, choosing $x \in \chi$. with probability $\frac{D(x^2)Q_l}{\sum_{x\in X} D(x)^2}$. , let D(x) denote the shortest distance from a data point to the closest center we have already chosen
3. Repeat Step 2. until we have taken k centers altogether.
4. For each i ∈ {1,...,k}, set the cluster C_i to be the set of points in X that are closer to c_i than they are to c_j for all j= i. 3. For each i ∈ {1,...,k}, set c_i to be the center of mass of all points in C_i.
5. Repeat Steps 3 and 4 until C no longer changes.

B. Optimal Cluster Number Determination

To determine the optimal number of well clusters, we use Silhouette Values as guidance. Note that engineering judgment is still needed to choose adequate cluster configuration for very dispersed well locations, as clustering algorithms can give different results for each iteration due to initial random cluster seeding. The silhouette value for each point measures how similar it is to points in its cluster compared to points in other clusters; hence it is a good metric to measure cluster distribution.

Journal of Earth Energy Engineering
Vol. 11 No. 3, December 2022, pp 113-124

The silhouette value S_i for the i^{th} point is defined as (Kaufman & Rousseeuw, 1990)

$$S_i = \frac{b_i - a_i}{\max{(a_i, b_i)}} \tag{8}$$

where a_i is the average distance from the ith point to the other points in the same cluster as i, and b_i is the minimum average distance from the ith point to points in a different cluster, minimized over clusters.

The silhouette value ranges from –1 to 1. A high silhouette value indicates that is well matched to its own cluster and poorly matched to other clusters . The clustering solution is appropriate if most points have a high silhouette value. If many points have a low or negative silhouette value, the clustering solution might have too many or too few clusters. With any distance metric, silhouette values can be used as an evaluation criterion for clustering.

Field Case Study

K Field is an oilfield located in South Sumatra, Indonesia. Major oil production contribution came from reefal carbonates with a minor contribution from sandstone layer. Fluid type in K Field is considered as black oil with API gravity of 38^o API. The reservoir is comprised of a single continuous zone with minor faults existence. The carbonates layer have good reservoir quality except in several local areas where tight facies occur, providing a permeability barrier and stratigraphic entrapment exceeding the simple four-way structural closures. In contrast, the sandstone reservoirs are rather tight.

The K Field is in peripheral waterflooding after its primary recovery. Wellcount in K-Field is at 383 production wells which can be divided into 61 groups. In this study, we will only consider an isolated well group that consists of 58 producer wells and 36 injection wells. The depth structure map for K-Field and wells locations is given in Figure 3. Production and injection rate data, including voidage replacement ratio (VRR) used in this study, are given in Figure 4a & 4b, respectively. VRR denotes the ratio between total injection and production rate, hence VRR values close to one imply that the flood is balanced. Figure 5 shows the average reservoir pressure.

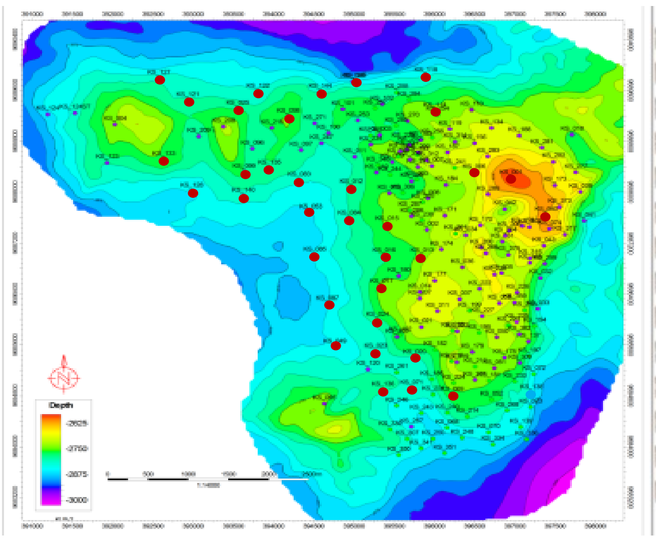

Figure 3. Depth Structure Map for Investigated Field (Red: Injector Wells, Purple: Producer Wells)

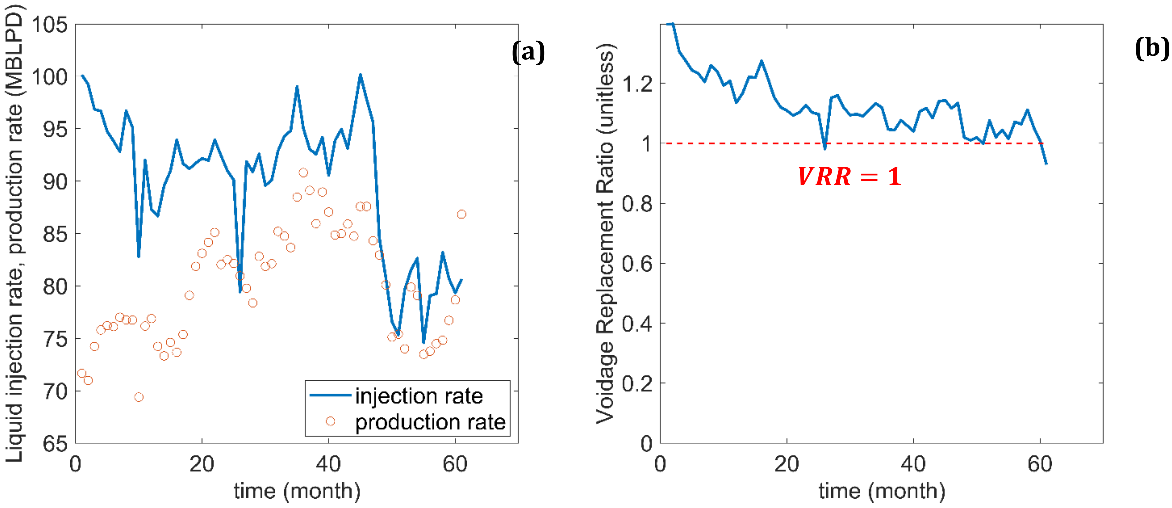

Figure 4. (a) Field Production and Injection Rate Data, (b) Voidage Replacement Ratio Plot

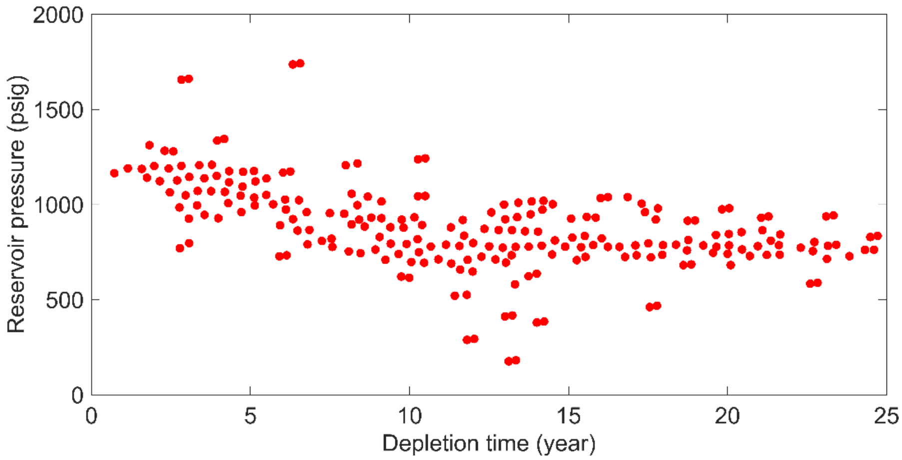

Figure 5. K-Field Average Reservoir Pressure

The VRR trend (Figure 4b) indicates a good balance between total injection and production rate as the values range between 1 – 1.2. Waterflood response is also clearly observed by comparing production rate changes as injection rates fluctuated from historical data (Figure 4a). As previously explained, having a rich response signal from rate data is essential for CRM calibration. Based on the VRR guide, the liquid rate history match in CRM will start from the 20th month. Log-log WOR-cum plot (Figure 6) showed that the criteria of frontal advance applicability had been reached for this field (Ershaghi & Abdassah, 1984).

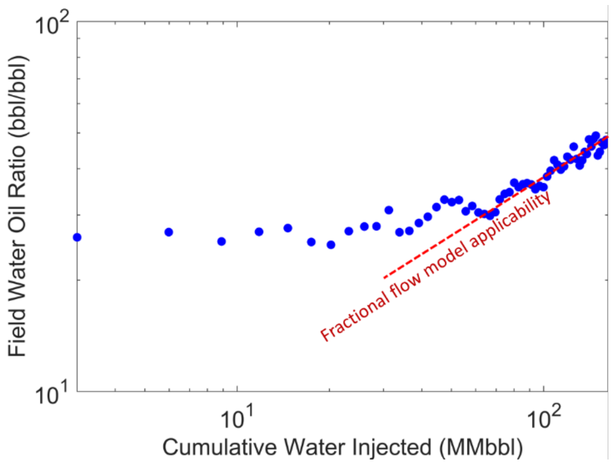

Figure 6. Log-log plot of Water Oil Ratio and Cumulative Water Injected from Field Data. Straight line trend obtained at the end of flood period denote the applicability range of empirical fractional flow model

Journal of Earth Energy Engineering
Vol. 11 No. 3, December 2022, pp 113-124

Bubble plots map can effectively aid in monitoring waterflood performance. This is especially important in the K field due to its peripheral nature. Several relevant bubble plot maps, such as cumulative oil produced, cumulative liquid produced, cumulative water injected, and liquid production rate, are given in Figure 7a and 7b, respectively. Due to all of the production wells being operated using an artificial lift, it is assumed that constant bottom-hole pressure approximation is suitable for this field.

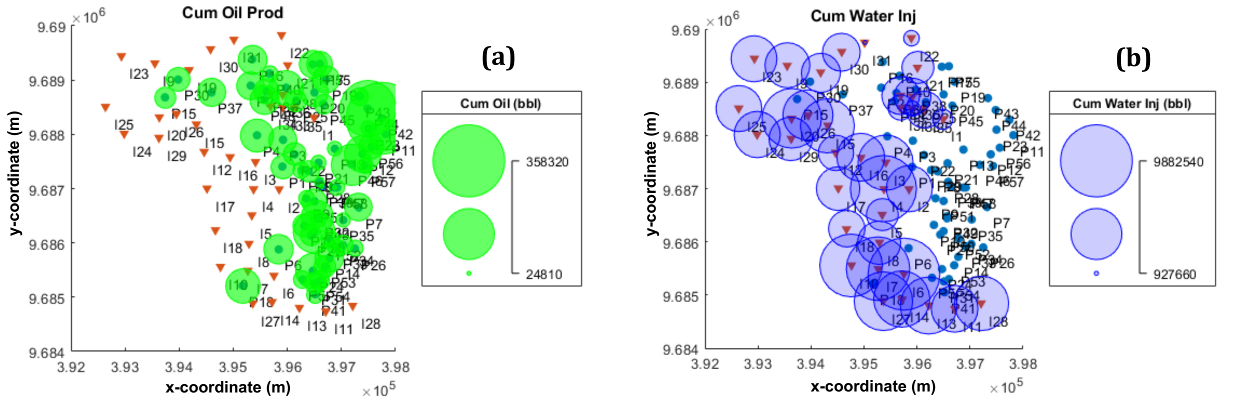

Figure 7. Bubble plot maps of (a) Cumulative oil produced, (b) Cumulative water injected

It can be observed from the bubble plot maps that water injection is quite equally distributed among all injectors. Another notable observation is that the highest oil-producer wells are located in the northeastern region, which is the furthest from injectors.

Due to CRM formulation, production data are preprocessed to be suitable for CRM input. Rate entries that show zero value (shut-in) are excluded from the input. Wells that have significantly low rates or have ceased to operate are also excluded. The prepared data are then used as input for CRM calibration and forecast to find the optimal allocation rate at the current injection capacity that delivers maximum cumulative oil produced.

RESULTS & DISCUSSIONS

Well Clustering

Based on silhouette values sensitivity, we find that six clusters ($k = 6$) are adequate to classify well groups in K-Field. Plots of well cluster distribution are given in Figure 8. We also provide clustering results using the general K-means algorithm for comparison. It can be inferred that weighted k-means++ gives a more balanced cluster and have closer centroids to the highest oil rate producers (see Figure 7a). Silhouette values of the K-Field cluster configuration are given in Figure 9.

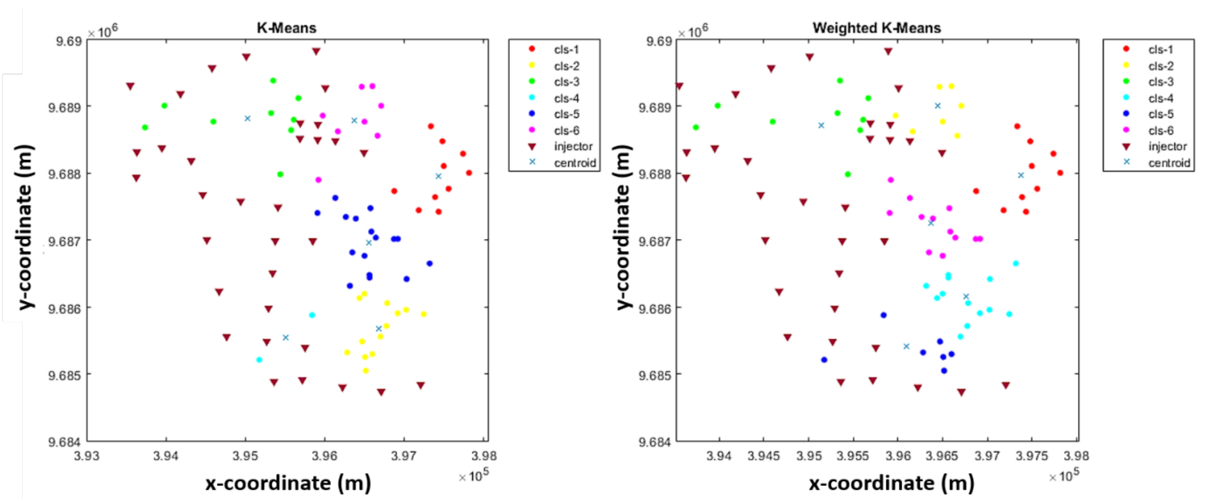

Figure 8. Clustering Result for Field K using six clusters ($k = 6$): with general K-means (left) and K-means++ with weighting (right)

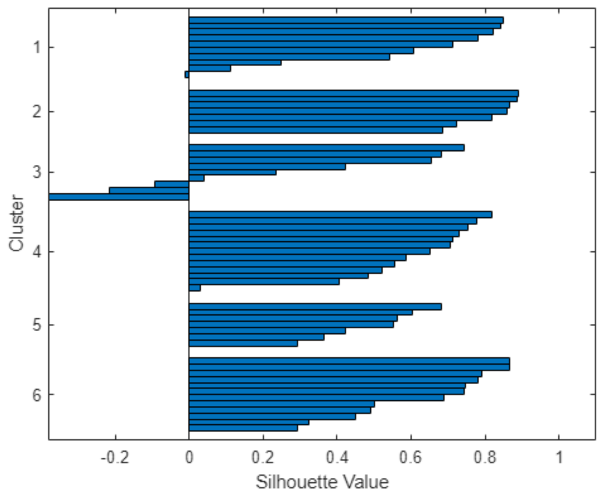

Figure 9. Silhouette Values of K-Field Clustering

History Match of Liquid and Oil Production Rates (CRM Calibration)

We performed a liquid rate history match to calibrate CRM-IPC time constants and cluster allocation factors. Figure 10 show the liquid rate comparison between calibrated CRM-IPC results and data at cluster levels. As per the previous discussion, the history-matched period started when the waterflood was balanced ($VRR \approx 1$). CRM-IPC liquid history match result is quite satisfactory and consistent with 'unclustered' CRM-IP. We obtain 18.2x increase in computation speed due to unknown parameters reduction from 52 wells to 6 clusters.

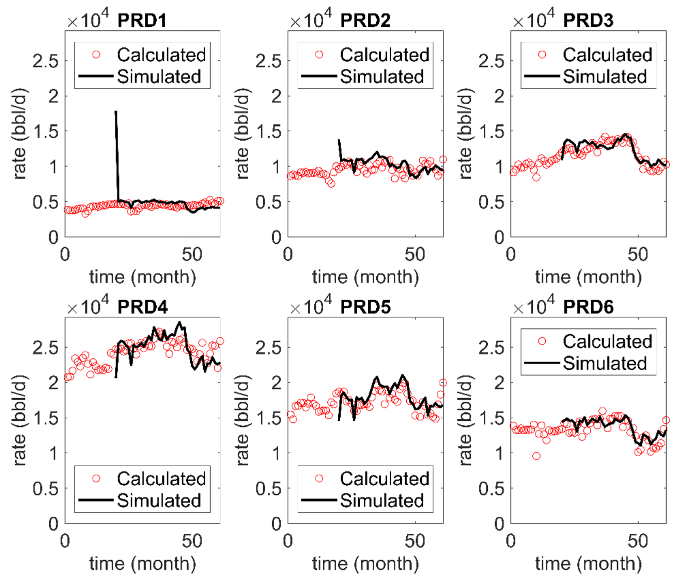

Figure 10. K-Field Cluster Liquid Rate History Match with CRM-IPC

Figure 11 show the oil rate history-match result for field level and cluster level, respectively, using CRM-IPC. The match result is generally quite satisfactory and faster than the original CRM-IP implementation on the same field (see Nugroho et al., 2021). However, we note that match results at a later period could be improved for a better forecast. Error (MSE) weighting at this later period is planned to alleviate this issue.

The CRM-IPC connectivity map is given in Figure 12. The arrow length represents allocation factor values from the injector to the connected producer. It can be inferred that the reservoir's northern part has stronger connectivity than its southern part.

Journal of Earth Energy Engineering
Vol. 11 No. 3, December 2022, pp 113-124

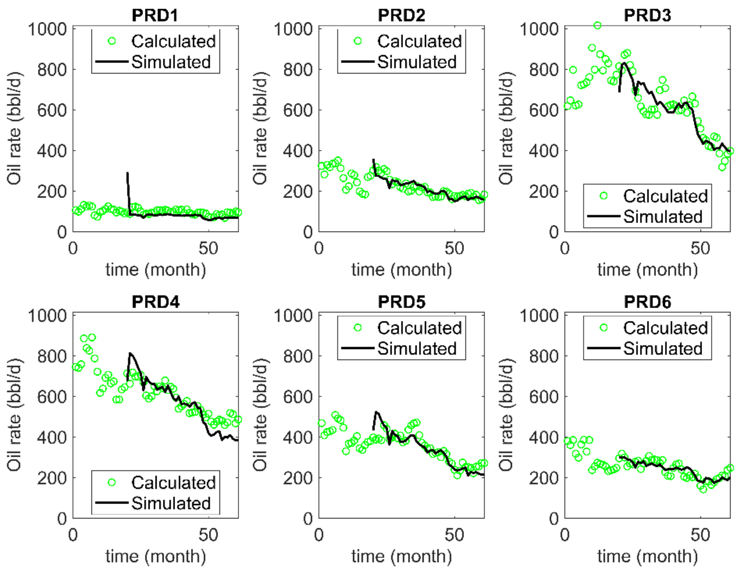

Figure 11. K-Field Cluster Oil Rate History Match with CRM-IPC

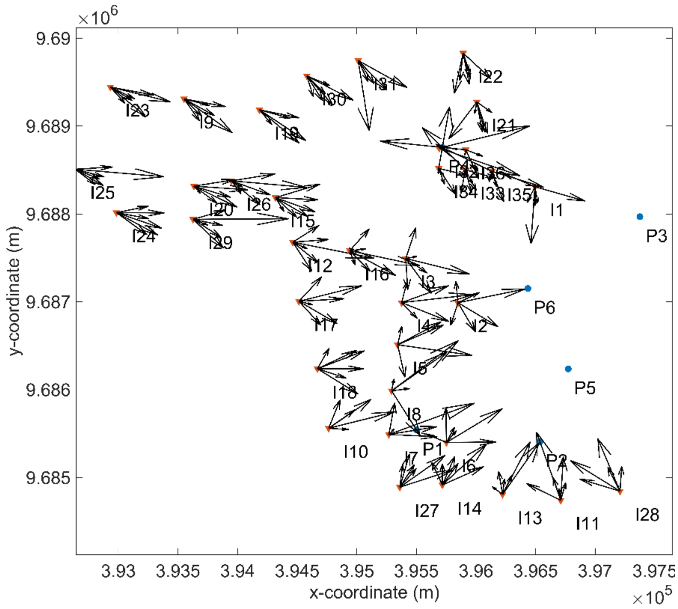

Figure 12. K-Field Connectivity Map from calibrated CRM-IPC

Prediction and Injection Allocation Optimization

After the CRM-IPC time constant and allocation factor has been calibrated. We performed a forecast of the waterflood performance for the base case (current allocation) and optimized the allocation scenario. It is assumed that total injection capacity is held constant, so the optimization will focus on how to reallocate water injection. A comparison of the forecasted oil rate and cumulative for both scenarios is given in Figure 13. By reallocating water injection, it is estimated that we will obtain 300 MSTB incremental oil gain in 10 years.

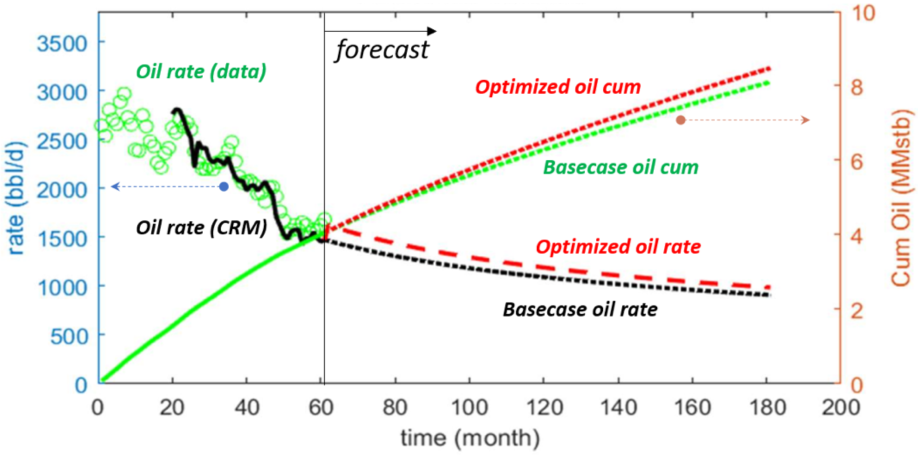

Figure 13. K-Field Base and Optimized Forecast. Constant total injection capacity case

To gain better comprehension visually, the average injection rate for each base and optimized the case in bubble maps were plotted (Figure 14). From this bubble map, we can observe that the injection rate is allocated more to northwest injectors. This optimization direction is automatically chosen due to higher connectivity in the northern part of the reservoir.

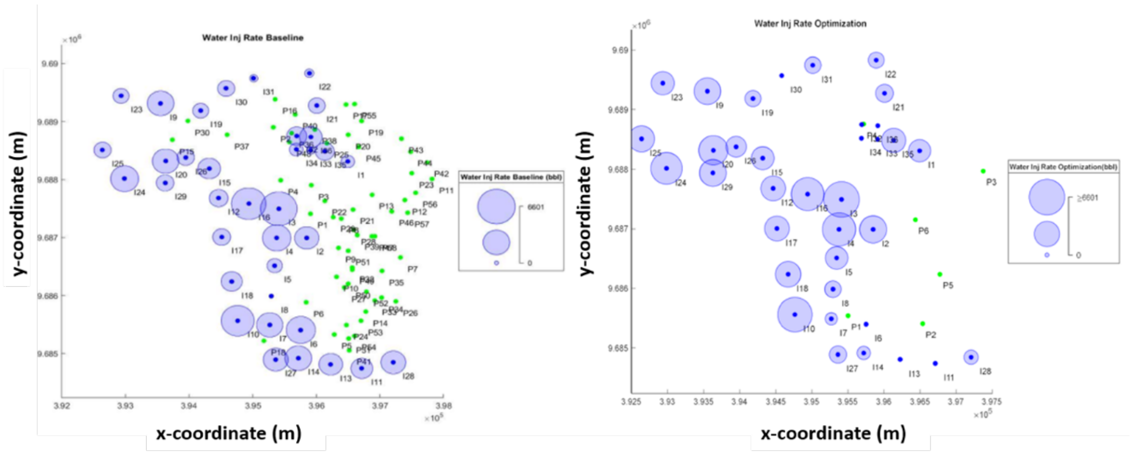

Figure 14. Bubble Map of Injection Rate Comparison with constant total injection capacity case: base case (left) and optimized allocation for clustered producer case (right)

CONCLUSIONS

Notable findings that we originated from this study are:

1. This study presents improved CRM-IP implementation for peripheral waterflooded fields with extensive injection and production wells by employing a clustering algorithm for well clustering. Well rate weighted k-means algorithm gives a more balanced cluster and has closer centroids to the highest liquid rate producers than the original k-means algorithm.
2. Based on the evaluated case study, CRM-IP with the clustering method gave up to 18 times faster computation time during model calibration (history match) than the original CRM-IP while retaining similar accuracy. Thus, it can improve CRM-IP applications for large-scale peripheral waterflood projects.
3. The radius of influence constraints to control clustering choice needs to be investigated in the future to avoid having a very dispersed production well cluster.

ACKNOWLEDGEMENTS

We acknowledge Ogrindo ITB Research Consortium members for the funding and permission to publish this work.

Journal of Earth Energy Engineering
Vol. 11 No. 3, December 2022, pp 113-124

APPENDIX A – Code/Software Availability

To implement the CRM-IPC practically and efficiently, we develop standalone desktop software for our code in a windows environment. This will allow the user to utilize the CRM-IPC implementation without needing a MATLAB® license. This software will be the starting point of the next improvement in our waterflood data-driven modeling research. The readers can access and modify the code through the github repositories: https://github.com/billalaslam/crmwaterflood_matlab.git

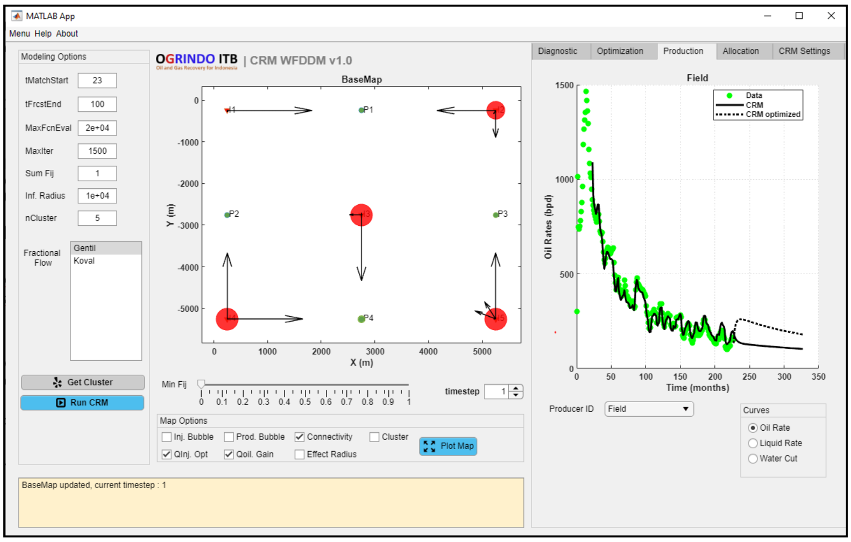

Figure 15. CRM WFDDM v1.0 Graphical User Interface (GUI)

REFERENCES

Albertoni, A., & Lake, L. W. (2003). Inferring Interwell Connectivity Only From Well-Rate Fluctuations in Waterfloods. *SPE Reservoir Evaluation & Engineering*, *6*(01), 6–16. https://doi.org/10.2118/83381-PA

Arthur, D., & Vassilvitskii, S. (2007). k-means++: the advantages of careful seeding. *SODA '07: Proceedings of the Eighteenth Annual ACM-SIAM Symposium on Discrete Algorithms*, 1027–1035. https://dl.acm.org/doi/10.5555/1283383.1283494

Artun, E. (2017). Characterizing interwell connectivity in waterflooded reservoirs using data-driven and reduced-physics models: A comparative study. *Neural Computing and Applications*, *28*(7), 1729–1743. https://doi.org/10.1007/S00521-015-2152-0/METRICS

Balaji, K., Rabiei, M., Suicmez, V., Canbaz, H., Agharzeyva, Z., Tek, S., Bulut, U., & Temizel, C. (2018, June 11). Status of Data-Driven Methods and their Applications in Oil and Gas Industry. *SPE Europec Featured at 80th EAGE Conference and Exhibition 2018*. https://doi.org/10.2118/190812-MS

Byrd, R. H., Hribar, M. E., & Nocedal, J. (1999). An Interior Point Algorithm for Large-Scale Nonlinear Programming. *SIAM Journal on Optimization*, *9*(4), 877–900. https://doi.org/10.1137/S1052623497325107

Davudov, D., Malkov, A., & Venkatraman, A. (2020, August 30). Integration of Capacitance Resistance Model with Reservoir Simulation. *SPE Symposium on Improved Oil Recovery*. https://doi.org/10.2118/200332-MS

Ershaghi, I., & Abdassah, D. (1984). A Prediction Technique for Immiscible Processes Using Field Performance Data (includes associated papers 13392, 13793, 15146 and 19506). *Journal of Petroleum Technology*, *36*(04), 664–670. https://doi.org/10.2118/10068-PA

Gentil, P. H. (2005). *The Use of Multilinear Regression Models in Patterned Waterfloods: Physical Meaning of the Regression Coefficients* [The University of Texas at Austin]. https://repositories.lib.utexas.edu/handle/2152/81125

Gildin, E., & Lopez, T. J. (2011). Closed-Loop Reservoir Management: Do We Need Complex Models? *SPE Digital Energy Conference and Exhibition*, 509–519. https://doi.org/10.2118/144336-MS

Guo, Z., Reynolds, A. C., & Zhao, H. (2018). Waterflooding optimization with the INSIM-FT data-driven model. *Computational Geosciences*, *22*(3), 745–761. https://doi.org/10.1007/S10596-018-9723-Y/METRICS

JAMALI, A., & ETTEHADTAVAKKOL, A. (2017). Application of capacitance resistance models to determining interwell connectivity of large-scale mature oil fields. *Petroleum Exploration and Development*, *44*(1), 132–138. https://doi.org/10.1016/S1876-3804(17)30017-4

Kaufman, L., & Rousseeuw, P. J. (1990). *Finding Groups in Data: An Introduction to Cluster Analysis* (L. Kaufman & P. J. Rousseeuw, Eds.). John Wiley & Sons, Inc. https://doi.org/10.1002/9780470316801

Kiær, A., Lødøen, O. P., de Bruin, W., Barros, E., & Leeuwenburgh, O. (2020). Evaluation of a data-driven flow network model (flownet) for reservoir prediction and optimization. *ECMOR 2020 - 17th European Conference on the Mathematics of Oil Recovery*, *2020*(1), 1–18. https://doi.org/10.3997/2214-4609.202035099/CITE/REFWORKS

Liu, H. H., Zhang, J., Liang, F., Temizel, C., Basri, M. A., & Mesdour, R. (2021). Incorporation of Physics into Machine Learning for Production Prediction from Unconventional Reservoirs: A Brief Review of the Gray-Box Approach. *SPE Reservoir Evaluation & Engineering*, *24*(04), 847–858. https://doi.org/10.2118/205520-PA

Møyner, O., Krogstad, S., & Lie, K. A. (2015). The Application of Flow Diagnostics for Reservoir Management. *SPE Journal*, *20*(02), 306–323. https://doi.org/10.2118/171557-PA

Nguyen, A. P., Kim, J. S., Lake, L. W., Edgar, T. F., & Haynes, B. (2011). Integrated Capacitance Resistive Model for Reservoir Characterization in Primary and Secondary Recovery. *SPE Annual Technical Conference and Exhibition*, *5*, 4162–4181. https://doi.org/10.2118/147344-MS

Sayarpour, M., Zuluaga, E., Kabir, C. S., & Lake, L. W. (2009). The use of capacitance–resistance models for rapid estimation of waterflood performance and optimization. *Journal of Petroleum Science and Engineering*, *69*(3–4), 227–238. https://doi.org/10.1016/J.PETROL.2009.09.006

Temizel, C., Energy, A., Nabizadeh, M., Kadkhodaei, N., Ranjith, R., Suhag, A., Balaji, K., & Dhannoon, D. (2017, May 9). Data-Driven Optimization of Injection/Production in Waterflood Operations. *SPE Intelligent Oil and Gas Symposium 2017*. https://doi.org/10.2118/187468-MS

Thakur, G. C. (1991). Waterflood surveillance Techniques - A Reservoir Management Approach. *Journal of Petroleum Technology*, *43*(10), 1180–1188. https://doi.org/10.2118/23471-PA

Thakur, G. C. (1998). The Role of Reservoir Management in Carbonate Waterfloods. *The SPE India Oil and Gas Conference and Exhibition*, *56*, 20–34. https://doi.org/10.2118/39519-MS

Wang, Z., He, J., Milliken, W. J., & Wen, X. H. (2021). Fast History Matching and Optimization Using a Novel Physics-Based Data-Driven Model: An Application to a Diatomite Reservoir. *SPE Journal*, *26*(06), 4089–4108. https://doi.org/10.2118/200772-PA

Weber, D., Edgar, T. F., Lake, L. W., Lasdon, L., Kawas, S., & Sayarpour, M. (2009). Improvements in Capacitance-Resistive Modeling and Optimization of Large Scale Reservoirs. *SPE Western Regional Meeting*, 369–385. https://doi.org/10.2118/121299-MS

Willhite, G. P. (1986). Waterflooding. In *Waterflooding*. Society of Petroleum Engineers. https://doi.org/10.2118/9781555630058

Yousef, A. A., Gentil, P., Jensen, J. L., & Lake, L. W. (2006). A Capacitance Model To Infer Interwell Connectivity From Production- and Injection-Rate Fluctuations. *SPE Reservoir Evaluation & Engineering*, *9*(06), 630–646. https://doi.org/10.2118/95322-PA

Zhao, H., Kang, Z., Zhang, X., Sun, H., Cao, L., & Reynolds, A. C. (2015, February 23). INSIM: A Data-Driven Model for History Matching and Prediction for Waterflooding Monitoring and Management with a Field Application. *SPE Reservoir Simulation Symposium*.

Zitha, P., Felder, R., Zornes, D., Brown, K., & Mohanty, K. (n.d.). *Increasing Hydrocarbon Recovery Factors*. Retrieved December 22, 2022, from https://www.spe.org/en/industry/increasing-hydrocarbon-recovery-factors/